

See discussions, stats, and author profiles for this publication at: <https://www.researchgate.net/publication/231693609>

Thermoreversible Gelation in Poly(diphenylsiloxane)/Diphenyl Ether Systems Exhibiting Mesophase Behavior

ARTICLE *in* MACROMOLECULES · JANUARY 2002

Impact Factor: 5.8 · DOI: 10.1021/ma0109673

CITATIONS

8

READS

12

4 AUTHORS, INCLUDING:



V. S. Papkov

Russian Academy of Sciences

134 PUBLICATIONS 897 CITATIONS

SEE PROFILE



Mikhail I. Buzin

Russian Academy of Sciences

96 PUBLICATIONS 311 CITATIONS

SEE PROFILE

Thermoreversible Gelation in Poly(diphenylsiloxane)/Diphenyl Ether Systems Exhibiting Mesophase Behavior

V. S. Papkov,* M. I. Buzin, M. V. Gerasimov, and E. S. Obolonkova

Nesmeyanov Institute of Organoelement Compounds, Russian Academy of Sciences, Vavilov str., 28, 119991 Moscow, Russia

Received June 4, 2001; Revised Manuscript Received October 30, 2001

ABSTRACT: The structural features and the thermodynamics of melting of thermally reversible gels of poly(diphenylsiloxane) (PDPhS) formed from 1.5 to 85 wt % solutions in diphenyl ether (DPhE) have been studied by means of differential scanning calorimetry, X-ray diffraction, and electron scanning microscopy. It was established that gelation occurs as a consequence of the crystallization of PDPhS that leads to a specific spherulitic morphology; i.e., overlapped spherulite-like superstructures, which are composed of lamellar crystallites, form a three-dimensional skeleton filled with the solvent. The phase diagram of the PDPhS/DPhE system was constructed. Its particular feature, resulting from the crystal–mesophase transition in the undiluted PDPhS, is interference between the crystal–isotropic solution and the thermotropic mesophase–isotropic solution equilibrium. The equilibrium temperature T_m° and the heat ΔH_m° of a virtual crystal–isotropic melt transition in PDPhS in the absence of solvent were estimated (280 °C and 10.34 kJ mol⁻¹) through use of the Flory equation when taking the melting temperatures of the annealed gels as the equilibrium melting points of PDPhS crystals in the presence of DPhE. The isotropization temperature (~560 °C) of the mesophase, which cannot be measured experimentally because of PDPhS thermal degradation, was assessed by extrapolation of the mesophase–isotropic solution boundary curve on the phase diagram of the PDPhS/DPhE system to the 100% polymer concentration. Phase diagrams expected for the system solvent–crystalline flexible/semirigid-chain polymer, exhibiting a crystal–mesophase transition, were schematically considered and compared to that of the PDPhS/DPhE system. On the basis of this consideration, the conclusion was drawn that the mesophase behavior of PDPhS is connected, at least in part, with a relatively high stiffness of its macromolecules.

Introduction

Poly(diphenylsiloxane) (PDPhS) has drawn attention for years as a polymer possessing enhanced thermal and oxidative stability.¹ Interest in this polymer has quickened in the past decade due to its thermotropic mesophase behavior.² However, considerable difficulties in synthesizing high molecular weight PDPhS, which is thermodynamically unstable, hindered its comprehensive investigation. Earlier studies on the thermodynamic characteristics³ and structure⁴ of the crystalline phase in PDPhS were performed using rather low molecular weight samples. Recently, we have shown that high molecular weight PDPhS can be prepared by anionic solid-state polymerization of hexaphenylcyclotrisiloxane.⁵ This method opens up new opportunities for further detailed investigation of this polymer. In particular, the crystalline structure⁶ was refined and rheological properties in the mesophase state were measured.⁷

Highly crystalline PDPhS exhibits a crystal–mesophase transition at about 260 °C.^{2b,5,8,9} The isotropization temperature T_i of PDPhS is above the onset of its thermal degradation and cannot be measured experimentally. High molecular weight PDPhS is soluble only in high boiling solvents such as diphenyl ether (DPhE), *o*-dichlorobenzene, and 1-chloronaphthalene at temperatures higher than 150 °C. Nevertheless, investigation of PDPhS solutions is undoubtedly of academic and technical application interest.

The addition of diluent to a crystallizable polymer reduces the melting point and this phenomenon under-

lies the approach to determining the equilibrium melting point and heat of fusion.¹⁰ The reported pertinent data for PDPhS³ were obtained on the low molecular weight samples and without regard to its mesophase behavior. Thus, it seemed to us quite reasonable to return to this problem and carry out a more detailed investigation in order to refine the reported and gain new data on thermodynamic parameters of the phase transitions in PDPhS using high molecular weight samples and currently available information about this polymer. This was one of the aims of the given work.

Another aspect of our investigation is gelation accompanying crystallization in PDPhS solutions. It is of importance both for a better insight into this phenomenon in polymers and in searching effective routes to purification of PDPhS and its processing. In principle, the formation of thermally reversible gels due to crystallization of polymer from solutions is a well-known and extensively discussed phenomenon, e.g. refs 11 and 12. Most of such gels are formed with slightly crystallizable macromolecules which contain a sufficiently large number of irregularities, i.e., comonomer units in copolymers and various defective monomer units in homopolymers (e.g., poly(vinyl chloride),¹³ poly(vinyl alcohol),¹⁴ branched¹⁵ and chlorinated¹⁶ polyethylene, ethylene–vinyl acetate copolymer¹⁷). The morphology of such gels in a simplified manner can be described by the often postulated fringed micelle model, i.e., crystallites of small sizes, formed by regular sequences in macromolecules, bind together irregular portions of chains into a three-dimensional network.

Crystallization of stereoregular homopolymers from dilute and moderately dilute solutions yields, as a rule,

* Corresponding author: e-mail vspap@ineos.ac.ru.

precipitated crystalline phases of different morphology. The morphology depends on solution concentration, temperature, and the type of phase separation, i.e., whether the crystallization occurs directly from homogeneous solution or a liquid–liquid demixing precedes it.¹⁸ Meanwhile, there are several prominent examples of the formation of thermoreversible crystalline gels by stereoregular polymers, in particular in such binary systems as isotactic polystyrene–decalin,¹⁹ linear polyethylene–xylene,^{20,21} poly(ethylene oxide)–xylene,²¹ and poly(4-methyl-1-pentene)–cyclohexane.²²

A prerequisite of gelation from the polystyrene solutions was suggested to be crystallization in the crystalline modification that can lead to fringed micellar crystallites.¹⁹ The gelation of poly(4-methyl-1-pentene) in cyclohexane solutions demonstrates in a striking fashion the gel structure of another type. In this system gels are formed by linked crystalline spherulites filled with the solvent. According to Mandelkern et al.,²¹ such a type of morphology, which results from the three-dimensional growth, impingement, and joining of well-organized spherulite-like superstructures, comprising crystals with lamellar habit, should be common for the gels formed by homopolymers (and even by copolymers with a low counits content) in dilute solutions.

We have found that gelation in the PDPhS/DPhE system is an interesting example of crystallization leading to a similar spherulite-like morphology. The study of these gels was the second objective of our work.

In this paper we present data on the formation and melting of PDPhS/DPhE gels and their morphology obtained using differential scanning calorimetry (DSC), X-ray diffraction, and scanning electron microscopy (SEM). On the basis of these data, the phase behavior of the PDPhS/DPhE system at different concentrations and temperatures is analyzed and the thermodynamic properties of the crystalline and mesomorphic phases in PDPhS are determined.

Experimental Section

PDPhS was synthesized by anionic solid-state polymerization of hexaphenylcyclotrisiloxane and freed from the initiator of polymerization following the reported procedure.⁵ Two PDPhS samples, i.e., PDPhS-A with specific viscosity 2.4 in 1% solution in DPhE at 145 °C ($M_w = 727\,000$, $M_w/M_n = 2.7$ according to GPC data based on polystyrene standards; measured on a Waters 150-C chromatograph at 135 °C using 0.04 wt % *o*-dichlorobenzene solutions⁵) and PDPhS-B with specific viscosity 0.75 were used. Commercially available DPhE was purified by recrystallization from melt prior use (mp 28 °C, bp 259 °C).

Solutions of PDPhS in DPhE with concentration from 1.5 to 50 wt % were prepared by heating corresponding mixtures in sealed tubes at 300 °C. Solutions of higher concentration were produced by evaporation of a corresponding amount of DPhE from the 20% solution. Upon natural cooling of the solutions, turbid coherent gels formed pervading all the solution volume. These virgin gels served as initial samples for all the performed measurements. Dried gels were prepared from them by extraction of DPhE with boiling acetone in a Soxhlet apparatus and subsequent drying in a vacuum.

The volume fraction in the gels at a given temperature was calculated with consideration for thermal expansion of both components. The density of DPhE ρ_s in the temperature range from 200 to 300 °C was estimated through use of the following empirical relationship derived from the density data available in the literature:²³

$$\rho_s = 0.884 + 7 \times 10^{-4}(250 - t)$$

where t is in °C.

As the density of amorphous PDPhS cannot be measured due to its thermal degradation, we used that of the mesophase, ρ_m , which was deduced from the reported data on linear dilatometry⁶ according to the following relationship:

$$\rho_m = 1.03 + 5 \times 10^{-4}(270 - t)$$

DSC measurements were performed on a DSM-3 calorimeter (Biopribor, Puschino, Russia) at a heating/cooling rate of 8 °C/min using ~20 mg gel samples placed in sealed aluminum pans. The presented below values of the heat of gel melting and gelation are the averages of several successive measurements, at least seven in the region of gel concentration below 10% where the monitored heats of transition were about 1 J g⁻¹.

X-ray diffractograms of gels were obtained on a DRON-3 diffractometer (Russia) fitted with a heater and temperature controller within ± 2 °C. Wet gel samples were placed in sealed special thin-walled capillary tubes. Nickel-filtered Cu K α radiation was used.

Optical experiments were carried out using a polarizing microscope equipped with a hot stage and photographic unit. The maximum temperature of observations was 350 °C. Gel samples were placed in sealed thin-walled containers with a rectangular cross section. SEM studies of the dried PDPhS gels were performed on a Hitachi-S-590 scanning microscope operated at 20 kV. Two kinds of dried gel samples were investigated. Dried gels from PDPhS-A were prepared using a freeze-drying method. A wet gel sample, placed on a substrate, was quenched in liquid nitrogen and then the solvent was sublimated under vacuum in a special device upon heating to room temperature for 12 h. We suggested that such a procedure had the least effect on the original morphology of the gel. Dried gels from PDPhS-B were obtained by extraction of DPhE with acetone as described above.

Results

Differential Scanning Calorimetry. We have investigated the phase behavior of PDPhS-A/DPhE systems with the polymer weight fraction w_2 up to 0.85. Starting with $w_2 \approx 0.015$, mechanically stable thermoreversible turbid gels are formed upon cooling transparent homogeneous solutions. X-ray diffraction has revealed a crystalline structure of these gels (see below). Melting of the gels on heating manifested itself as the occurrence of an endotherm on DSC traces extended over a certain temperature interval (see Figure 1). Optical observations under polarizing microscope showed that at the same temperatures the gels with $w_2 < 0.8$ converted directly into homogeneous solutions. Their subsequent cooling led in turn to a heat evolution accompanied by the appearance of birefringent domains. At $w_2 \geq 0.8$ the melting of gels occurred in a more complex manner: formation of isotropic solutions followed the previous transformation of the crystalline phase into the mesophase. This phenomenon will be described in more detailed below (see section "Isotropization").

The dependencies of the gel melting temperature T_m and the gelation temperature, assigned further as the crystallization temperature T_c , on the content of PDPhS in gels are shown in Figure 2. Locating the end of melting endotherms and the onset of crystallization exotherms on DSC curves is a rather problematic procedure (especially in the case of retarded kinetics of dissolution and gelation of high molecular weight polymers with a wide molecular weight distribution). Therefore, we have taken the melting and crystallization peak temperatures as the T_m and T_c . In Figure 2 T_m are given, which were monitored in the second DSC runs

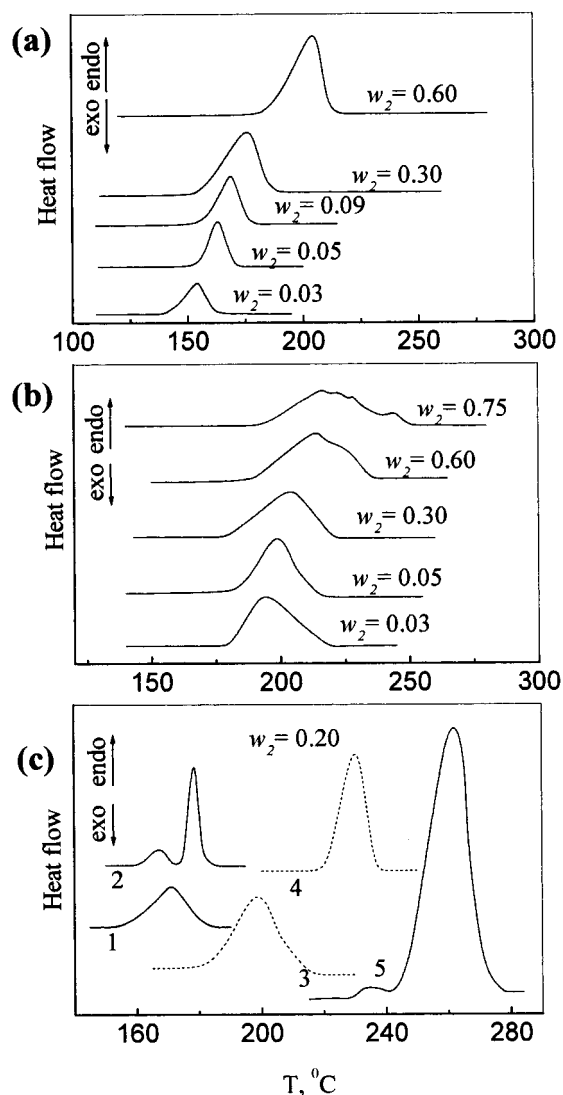


Figure 1. DSC traces of PDPhS/DPhE gels with various polymer weight fraction w_2 . (a) Wet gels formed upon cooling with a cooling rate of 8 °C/min. (b) Dried gels prepared from their wet precursors formed upon fast cooling. (c) Wet and dried gels with $w_2 = 0.2$: (1) virgin wet gel; (2) wet gel annealed at 165 °C for 1 h; (3) dried virgin gel; (4) dried annealed gel; (5) dried gel after annealing at 300 °C. Heating rate 8 °C/min.

after the virgin gel samples, obtained as described in Experimental Section, were melted in the calorimeter during the first heating run and then cooled with a cooling rate of 8 °C. Upon cooling the gelation, crystallization occurred at the temperatures lower by 20–50 °C than T_m of the gels. At the polymer weight fraction below 0.2, T_c and T_m decreased quite sharply in a similar manner. Annealing the gels at temperatures close to the onset of the melting peaks led to an increase in T_m on subsequent heating, especially considerable at w_2 below 0.2 (see Figures 1c and 2).

Dried virgin gels exhibited on heating the crystal–mesophase transition at 200–210 °C (DSC peak temperatures in Figures 1b and 2). Note that at the high contents of PDPhS in parent wet gels the endotherms of this crystal–mesophase transition on the DSC traces are spread over a rather wide temperature range, and some of them are even multiple (Figure 1b). This points to the occurrence of a partial perfection of some crystallites, which proceeded at higher gelation tempera-

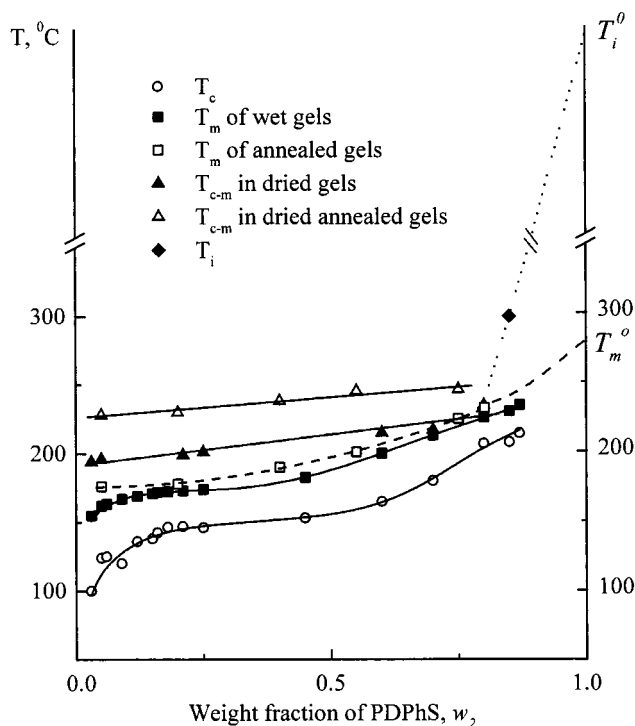


Figure 2. Temperatures of gelation–crystallization (T_c), gel melting (T_m), crystal–mesophase transition (T_{c-m}) and isotropization [mesophase dissolution] (T_i) as a function of polymer weight fraction in PDPhS/DPhE wet and dried gels and solutions. Data points are the peak temperatures on DSC traces obtained at a heating/cooling rate of 8 °C/min. Annealing temperatures were lower by ~10 °C than T_m of initial wet gels (annealing time = 1 h). Dashed curve is calculated using eq 3 with $T_m^0 = 553$ K (280 °C), $\Delta H_m^0 = 10.34$ kJ mol⁻¹ (52.2 J g⁻¹), and $B = 8.8$ J cm⁻³ (see text). Dotted line is a schematic drawing of the mesophase–isotropic solution boundary curve (see text).

tures. In gels, dried after previous annealing, the temperature of this transition, T_{c-m} , increased by ~30 °C, and the transition peaks became single and considerably sharper (Figures 1c and 2).

The heat of melting/gelation of the wet gels ΔH_m vs polymer content is given in Figure 3. At $w_2 > 0.2$ a straight line can be fitted to the data points, whose extrapolation to $w_2 = 1$ yields the heat of fusion of the polymer crystalline phase formed at gelation (~13 J g⁻¹). In the polymer content range $w_2 = 0$ –0.2 this plot is a curve coming from the origin. In this region the heat of mixing of DPhE with PDPhS provides a perceptible contribution into the total heat of melting of the gels (see section “Thermodynamics of Melting”). The heat of crystal–mesophase transition ΔH_{c-m} was found to be practically constant for all the dried gels and equal on the average to 10.3 J g⁻¹. ΔH_{c-m} for dried samples obtained from the annealed gels was above, if any, this value by no more than 10%.

X-ray Data. The crystalline structure of the PDPhS gels was verified by X-ray diffraction. Figure 4 furnishes the X-ray diffractograms taken at various temperatures for some wet and dried gels with different content of PDPhS. A particular feature of the X-ray diffractograms of all the wet gels, taken at ambient temperature, is the existence of a diffraction peak at $2\Theta = 7^\circ$ – 10° (corresponding to the 7.01 nm d spacing) with more or less clear-cut shoulders at 9.4° and 10.5° in 2Θ ($d = 0.94$ and 0.84 nm). For the gels with $w_2 > 0.1$ there is a poorly resolved doublet in the region of larger diffrac-

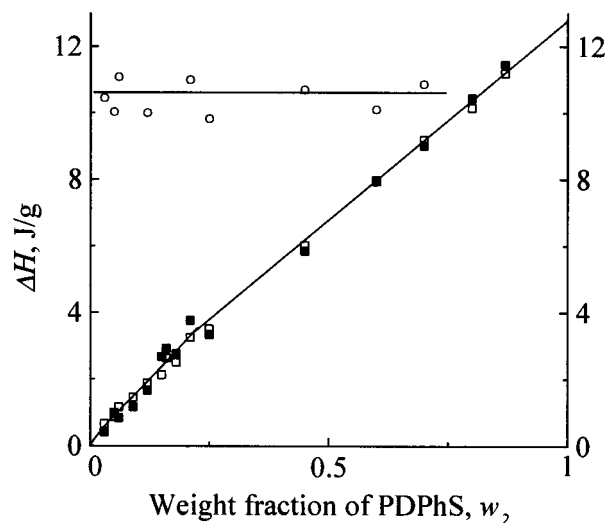


Figure 3. Heats of fusion of wet gels (■) and gelation-crystallization from solutions (□) and heat of the crystal-mesophase transition in dried gels (○) as a function of PDPhS weight fraction.

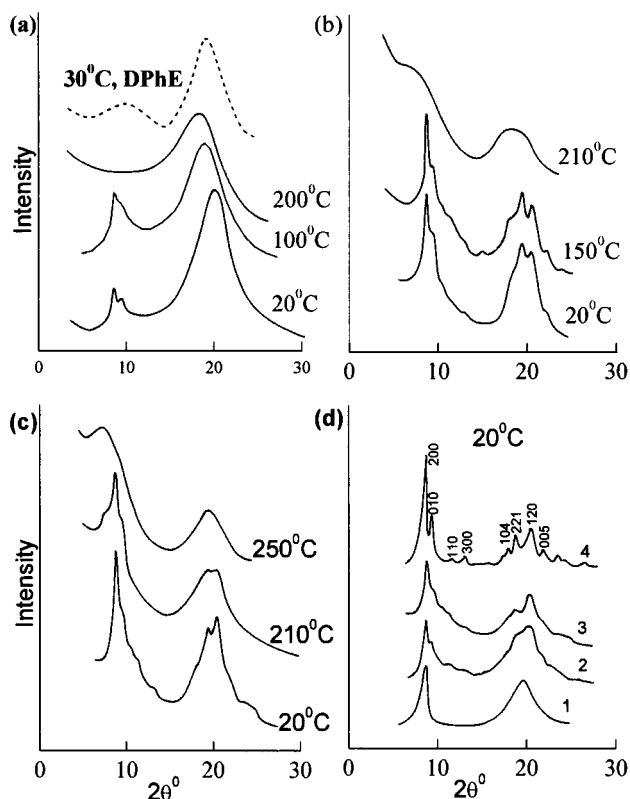


Figure 4. X-ray diffractograms taken at different temperatures for wet (a–c) and dried (d) gels with various PDPhS weight fraction w_2 : (a) $w_2 = 0.03$, the dotted curve is X-ray diffractogram of DPhE; (b) $w_2 = 0.20$; (c) $w_2 = 0.75$; (d) dried gels with initial $w_2 = 0.03$ (1), 0.10 (2), and 0.75 (3) and a gel annealed at 300 °C (4); the indices of reflections are indicated according to ref 6.

tion angles at 19°–19.5° and 20.5° 2 θ ($d = 0.455$ – 0.470 and 0.433 nm) which has two shoulders at ~18° and 22° 2 θ ($d = 0.492$ and 0.403 nm). Amorphous halo originated from X-ray scattering by molten DPhE molecules is located in the same region of diffraction angles. This is an intense halo (see Figure 4a) which, being superposed on the crystalline reflections of the PDPhS, obliterates the profile of the gels diffractograms,

especially strongly at low polymer concentrations. In Figure 4a this fact is illustrated by the diffractograms of a gel with $w_2 = 0.03$. In the range of diffraction angles from 16° up to 20°, there exists only one rather wide and intense diffraction peak, but the other crystalline reflections indicated above are indiscernible.

In the course of stepwise heating the gels all the above-listed crystalline reflections became more pronounced and, in addition, extra weak reflections appeared at ~11.5° and 13° 2 θ ($d = 0.77$ and 0.68 nm). Such changes in the diffractograms point to perfection of the initially formed crystalline phase, and this fact is in line with the observed increase in the gel melting temperature after annealing. As melting advances, the crystalline reflections gradually disappear, and in the diffractograms of the molten gels there exist only two amorphous halos centered at ~6° and 20° 2 θ . The location of the former is determined by the weight fraction of PDPhS, shifting to lower diffractions angles with decreasing polymer content in the gel. The intensity of this amorphous halo is increasing without any change of its position during gradual gel melting upon heating. These facts suggest that amorphous domains do not swell with DPhE to an appreciable extent in these crystalline gels. Coexistence of the crystalline phase of PDPhS and its solution in DPhE in the temperature range of melting is illustrated by the diffractogram of a gel with $w_2 = 0.75$ taken at 210 °C (Figure 4c). Upon subsequent cooling the solutions, which were formed after complete dissolving PDPhS, the initial profile of the diffractograms was always recovered.

The profile of the diffractograms of dried gels depends on the polymer weight fraction in the parent wet ones. The diffractograms of dried samples, prepared from wet gels with $w_2 = 0.03$, 0.1, and 0.75, are shown in Figure 4d. Dried gels with low initial content of PDPhS ($w_2 < 0.05$) exhibit diffractograms containing a single peak at ~8.8° 2 θ and also a wide one centered at ~20° 2 θ with hardly distinguishable shoulders. With increasing polymer content in the wet gels the second peak becomes more and more structured. Annealing of gels before drying led to the development of more clear-cut crystalline reflections.

In Figure 4d, the diffractogram is also presented for one of the dried gels that was annealed in the mesomorphic state at 300 °C for 2 h and then crystallized upon slow cooling. This is a sample with a very high degree of crystallinity (seemingly close to 1) and a heat of crystal-mesophase transition of 37 J g⁻¹ (see its DSC trace in Figure 1c). Its X-ray diffractogram corresponds to the earlier described monoclinic crystalline modification⁶ with unit cell parameters $a = 2.133$ nm, $b = 0.991$ nm, $c = 2.030$ nm, and $\gamma = 108.9^\circ$. Comparison of the X-ray diffractogram of this sample with those for the wet and dried gels shows that the peaks at 1.01, 0.94, 0.77, 0.68, 0.492, 0.470, 0.433, and 0.403 nm in the latter diffractograms can be associated with the (200), (010), (110), (110), (300), (104), (221), (120), and (005) reflections of the monoclinic crystal. A certain discrepancy in the location of some of these peaks and their more spread profiles can be attributed to a lower perfection and small sizes of crystallites in the gels as well as to an effect of X-ray scattering from amorphous domains. Unfortunately, it is practically impossible to estimate the amorphous phase content in the dry gels using their X-ray diffractogram patterns. The reason is that the first sufficiently sharp intense amorphous halo, which

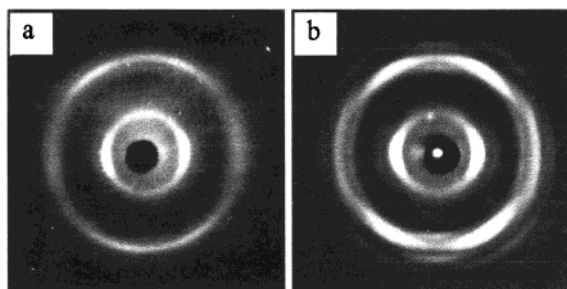


Figure 5. X-ray fiber patterns of oriented dried gels with an initial $w_2 = 0.03$ before (a) and after (b) annealing at 300 °C (reproduced from ref 6).

could likely be appropriate for this purpose, is positioned at the same diffraction angles as the crystalline reflections (200) and (010) (judging from the X-ray diffractogram of the molten PDPhS oligomer^{9a}). However, the existence of amorphous phase in the gels in about 0.7 weight fraction is evidenced by comparison of the heat of crystal–mesophase transition for all the dried gels ($\sim 10.3 \text{ J g}^{-1}$) with that of the above-mentioned sample of PDPhS crystallized upon cooling from the mesomorphic state (37 J g^{-1}). The earlier reported results of dynamic mechanical and dielectric measurements^{5b} also evidence the existence of amorphous phase in PDPhS samples with the low heats of the crystal–mesophase transition.

Earlier we have reported that the dried samples, which were prepared from gels with low PDPhS content and showed X-ray diffraction patterns similar to diffractogram (1) in Figure 4d, contained after coextrusion with lead at 150 °C the partially distorted tetragonal crystalline phase with unit cell parameters $a = 1.02 \text{ nm}$ and $c = 0.99 \text{ nm}$.⁶ The difference between the X-ray diffraction patterns of the oriented tetragonal and monoclinic crystalline phases can be seen from Figure 5. We suggest that upon coextrusion the monoclinic modification could convert into the tetragonal one. Nevertheless, we cannot completely exclude that on gelation a certain fraction of the tetragonal crystals is formed as well. Note, in this connection, that the most intense reflection observed in the X-ray patterns of the tetragonal crystalline phase are (100) and (102) with $d = 1.02$ and 0.445 nm ($2\theta = 8.66^\circ$ and 19.93°).⁶

Scanning Electron Microscopy. The scanning electron micrographs presented in Figure 6 reveal the morphology of the gels of PDPhS-A dried in a vacuum (see “Experimental Section”). The wet parent gels were obtained on self-cooling of solutions and had the melting temperatures close to those indicated in Figure 2. We can see that the gels possess well-organized spherulite-like superstructures overlapping with each other. Earlier, the similar morphology was already observed for polyethylene and poly(ethylene oxide) gels formed from xylene.^{20,21} Electron micrographs taken at low magnification show that with increasing polymer concentration in the initial solution spherulites become larger and their amount per unit volume of the formed gel decreases. For instance, the diameter of spherulites in gels with $w_2 = 0.07$, 0.20, and 0.75 was found to be ~ 10 , 30–50, and $\sim 60 \mu\text{m}$, respectively (Figure 6a,c,d). Such a trend may be explained by a larger number of primary crystalline nuclei in the course of the gelation–crystallization at lower temperatures, especially at $w_2 < 0.2$ (see Figure 2). This suggestion is supported by the fact that, upon slow cooling of the solutions of lower con-

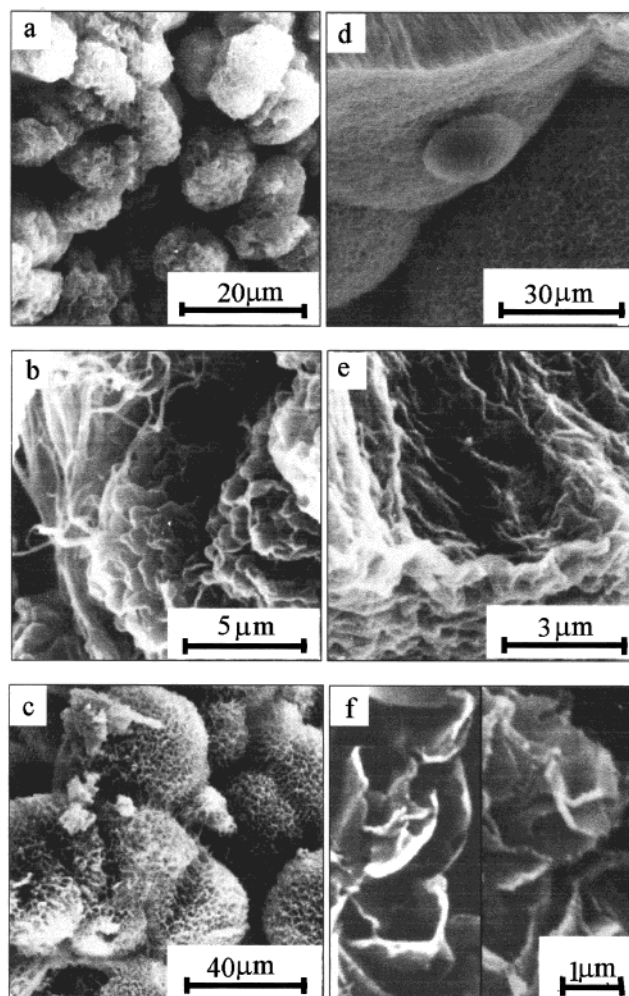


Figure 6. SEM micrographs of dried PDPhS-A gels with various initial $w_2 = 0.07$ (a, b), 0.20 (c), and 0.75 (d, e) and dried PDPhS-B gel with initial $w_2 = 0.05$ (f) before (left) and after (right) annealing at 300 °C for 1 h.

centration or their prolonged isothermal crystallization at higher temperatures, spherulites grow considerably larger in size. As an illustration, the optical photomicrograph of an intermediate stage of gelation from the 3 wt % solution, cooled very slowly to 105 °C, is given in Figure 7a.

The electron micrographs in Figure 6b,e,f, taken at high magnification, reveal the inner organization of the spherulites. They are cellular superstructures, consisting of slightly twisted crystalline lamellae that branch and join each other. In the gels with low polymer content the cellular skeleton is quite loose, but with increasing polymer content it becomes increasingly dense. The density of the inner part of spherulites (a characteristic inverse to the cell dimensions) is changing along the radius. Figure 6e shows that the outer layer of a spherulite in the gel with $w_2 = 0.75$ is more loose than its core. This is likely due to a gradual decrease in the solution concentration as the spherulite grows.

The lamellar thickness seems to be practically the same for all the gels independent of w_2 and equal to 80–100 nm. These values were derived from the width of the lateral faces of lamellae, which lie in the plane of the micrographs or are slightly inclined to it. It is noteworthy that no increase in the lamellar thickness was observed after annealing wet and dried gels even at temperatures above T_{c-m} . The electron micrographs

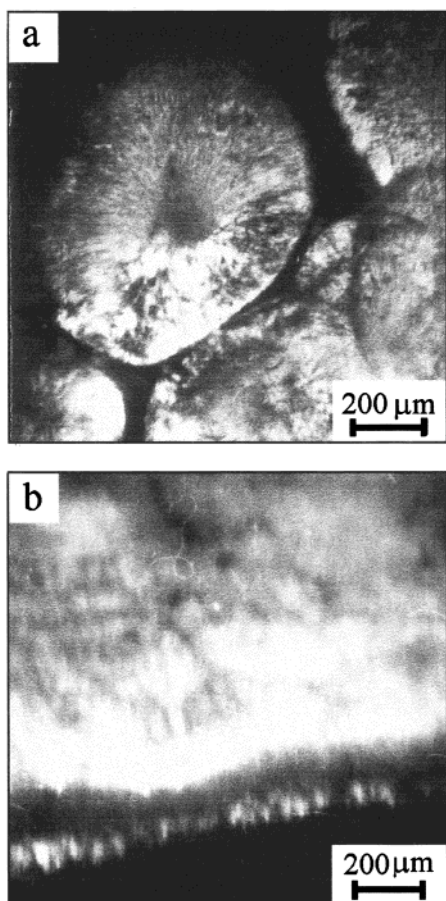


Figure 7. Optical photomicrographs of a 3 wt % solution of PDPhS-A, slowly cooled to 105 °C, at an intermediate stage of gelation (a) and of a 85 wt % heterogeneous solution of PDPhS-A, containing a birefringent mesophase, at 270 °C (b) (in polarized light; crossed polars).

of a PDPhS-B gel with $w_2 = 0.05$ before and after annealing at 300 °C (Figure 6f) are illustrative of this fact. Unlike the gels of PDPhS-A, this gel after extraction of DPhE with acetone did not retain integrity and consisted of fragments of broken spherulites and single twisted lamellae. The edges of some crumbled lamellae, especially after annealing, clearly show their inner striated structure that suggests the alignment of the macromolecular chains perpendicular to the end faces of the lamellae.

The thickness of 100 nm corresponds to a molecular weight of about 80 000 for the extended *cis-trans* conformation of the siloxane backbone (0.5 nm per $[-O-Si(C_6H_5)_2-]_2$ unit⁶). The molecular weight of PDPhS-A, estimated from GPC data using polystyrene standard, is about 720 000. The real molecular weight can be somewhat less, as PDPhS macromolecules appear to be more rigid than polystyrene ones. (According to the recent theoretical calculations, the “characteristic ratio” C for PDPhS macromolecules with high degrees of polymerization is ~ 60 at 300 °C.²⁴) Nevertheless, it is evident that the lamellae are built up from folded chains.

To summarize, formation of thermally reversible gels of PDPhS from DPhE solutions is a result of the growth and overlapping of spherulite-like superstructures consisting of crystalline folded chain lamellae. Being in a close contact, the spherulites build up a pervading all the volume, unified skeleton, which provides integrity

and elasticity of the gel. The mechanical properties of the gels are obviously determined by the type of contacts, the size, and inner structure of spherulites. Our tentative measurements of the modulus of elasticity in compression yielded values of 19.6 kPa and 2.1 MPa for the gels with $w_2 = 0.1$ and 0.5, respectively.

Discussion

Structure of Gels. Although the general concept of the spherulitic morphology is quite clear, the inner structure of spherulites calls for a more detailed consideration. The spherulite-like superstructures can apparently be treated as highly grown dendrites with relatively large longitudinal dimensions of their constituent lamellae ($\sim 1-3 \mu\text{m}$). Judging from the size of spherulites and their amount per unit volume of the gel, the number of the crystalline nuclei, on which the spherulites grow upon cooling, increases as the concentration of solution decreases (see Figure 6). This fact can apparently be explained by lower temperatures of gelation—crystallization from solutions of lower concentrations. The factors governing longitudinal dimensions of lamellae and the mechanism of their branching are not quite clear.

Another interesting issue is the inner lamellar structure. The fact that annealing leads to increasing both the gel melting temperature, especially pronounced for the gels with low polymer content, and the temperature of the crystal–mesophase transition in the absence of solvent (see Figure 2) implies that the crystalline lamellae initially growing from DPhE solutions are of low perfection. It is well-known that on crystallization of flexible polymers from dilute solution metastable lamellae grow which dissolve and melt at lower temperatures than those formed on crystallization from the melt²⁵ (see also ref 26 and references therein). Increase in the melting point of such lamellar crystals due to annealing is mainly connected with increasing chain fold. However, annealing of the wet PDPhS gels and the dry ones at the temperatures above T_{c-m} did not lead to any detectable change in the lamellar thickness. This means that the gel melting point T_m is determined not by the whole thickness of lamellae but only by the length of crystalline chain sequences in them, i.e., by the concentration of various defects and their distribution within lamellae. In principle, the well-known paracrystalline model of Hosemann²⁷ summarizes all possible defects to be expected in the crystalline PDPhS lamellae. The structure of a defective PDPhS lamella can supposedly be presented in a simplified fashion by a conventional two-phase model. The lamella with irregular chain folds consists of an outer amorphous layer (free chain ends and long chain loops) and a crystalline core in which small domains of conformationally disordered chain segments are randomly embedded interrupting the crystalline sequences of macromolecules. Recall that the estimated above content of amorphous phase in dried gels is about 0.7.

Let us speculate further how the concentration of solution can affect the inner organization of such crystalline lamellae in the case of their athermal primary nucleation. According to Hoffman’s nucleation theory,²⁸ the growth of a lamellar crystal proceeds via formation of secondary nuclei at its growing lateral face. Dimensions of the critical secondary nucleus are a function of the reciprocal of supercooling. On crystallization from the solution of a given concentration two

factors must be taken into account, which determine the supercooling required for experimentally reasonable rates of crystallization in a cooling regime used. These factors are (i) depression of the equilibrium melting point of the polymer in the presence of solvent, which can be described by the Flory equation,¹⁰ and (ii) influence of the polymer concentration in solution on the dimensions and kinetics of formation of secondary crystalline nuclei.

According to the theory, the width (a^*) and the length (l^*) of the critical secondary nucleus can be expressed as

$$\begin{aligned} a^* &= 4\gamma T_m^\circ / \Delta h \Delta T \rho_c \\ l^* &= 4\gamma_e T_m^\circ / \Delta h \Delta T \rho_c \end{aligned} \quad (1)$$

Here T_m° is the equilibrium melting point of the undiluted polymer, γ and γ_e are the side and end surface free energy, ΔT is the supercooling, and Δh and ρ_c are the specific heat of fusion and density of the crystal.

The formation of the nucleus with a transverse dimension $a^* = n^*d$ suggests the association of n^* macromolecules with diameter d . It is obvious that the rate of formation of such nuclei and thus the overall rate of crystallization should be a function of solution concentration and n , being at a given concentration the higher the less n . As a^* and, hence, n^* are inversely related to ΔT , commensurate rates of crystallization from solutions of different concentrations in the same cooling regime should be experimentally monitored at different temperatures, which are the lower the smaller the concentration. This appears to be a reason for the observed sharp decrease of the gelation–crystallization temperature at the polymer concentrations in solution below 0.2 (Figure 2). At the same time, the lower the crystallization temperature, the smaller is the critical nucleus length ($l^* = a^*\gamma_e/\gamma$). Within the framework of the model of PDPhS lamellae proposed above, this fact can explain the parallel drop in the melting temperature of the gels in the same range of concentration if one assumes that the length of crystalline sequences of macromolecules in the lamellae is determined by l^* .

Taking T_m of the annealed gels as the equilibrium melting temperature T_m^{eq} of the PDPhS lamellar crystals grown from solution, it is possible to assess tentatively the relation between the length of the secondary nucleus l^* and the final length of crystalline domains l in the lamellae grown at different gel formation temperatures. For this purpose, we used the theoretical relationship between T_m and T_c derived for crystallization from the melt²⁹

$$T_m = [T_m^{\text{eq}}(2\beta - 1) + T_c]/2\beta \quad (2)$$

where $\beta = l/l^*$. The plot of the calculated β against w_2 is presented in Figure 8. We can see that at the lowest temperatures of crystallization the length of crystalline domains in the lamellae is close to those of the critical crystalline nuclei. The significant increase in T_m of the gels with $w_2 > 0.4$ is likely connected not only with an expected increase in the length of the secondary nucleus but also with its subsequent lengthwise growth. Evidently, the above speculations are oversimplified, and the parameter β reflects in fact not only the nucleus lengthening in the course of crystallization but also different perfection of lamellae grown from solutions of various concentration and at different temperatures.

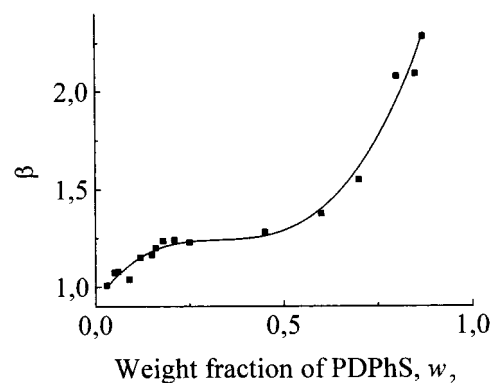


Figure 8. Parameter β in eq 2 as a function of PDPhS weight fraction in gels.

Thermodynamics of Melting. On the basis of the Flory approach, Takahashi et al.³⁰ have theoretically analyzed the effect of the crystal dimensions on the melting temperature of crystalline gels of copolymers and branched homopolymers. The relationships derived by these authors allow, in principle, to calculate the thermodynamic parameters of fusion of the crystalline phase if the size of gel crystallites and their interfacial free energy are known. However, the measurement of the crystallite sizes is often a very difficult experimental problem, and reliable data on the surface free energy are, as a rule, not available.

In our study we suggested that the crystals in the annealed gels gained perfection close enough to that of the equilibrium ones. Thus, we considered the melting temperature of these gels to be the equilibrium melting points of the crystalline phase of PDPhS in the presence of DPhE and used the Flory equation for estimating the equilibrium thermodynamic properties of the undiluted polymer

$$\frac{1}{T_m^{\text{eq}}} - \frac{1}{T_m^\circ} = \frac{R}{\Delta H_u^\circ} \frac{V_2}{V_1} \left(\phi_1 - \frac{BV_1}{RT_m^{\text{eq}}} \phi_1^2 \right) \quad (3)$$

where T_m° is the equilibrium melting point of the undiluted polymer, T_m^{eq} is the equilibrium melting temperature of crystallites in the presence of DPhE, ΔH_u° denotes the heat of fusion per polymer repeat unit [$\text{SiO}(\text{C}_6\text{H}_5)_2$], V_1 and V_2 stand for molar volume of the solvent and the polymer, ϕ_1 is the solvent volume fraction, and B represents the polymer–solvent interaction.

We solved a set of eqs 3, written for all the T_m^{eq} given in Figure 2, by means of the least-squares method and calculated $T_m^\circ = 553 \text{ K}$ (280°C), $\Delta H_u^\circ = 10.34 \text{ kJ mol}^{-1}$ (52.2 J g^{-1}), and $B = 8.8 \text{ J cm}^{-3}$ under the assumption that B is constant over the whole concentration range. As shown in Figure 2, the theoretical curve (dashed), computed using eq 3 with the above parameters, fits the experimental data rather well (with a standard deviation of 0.8 K).

Note that the crystalline phase in PDPhS does not melt in the absence of solvent but converts above 260°C into the mesophase, and the isotropization temperature cannot be attained experimentally due to the onset of thermal degradation at lower temperatures. Therefore, the calculated ΔH_u° and T_m° are conceptually the enthalpy and temperature of a virtual transition from the crystalline phase into an imaginary isotropic melt. Consequently, ΔH_u° should include the heat of

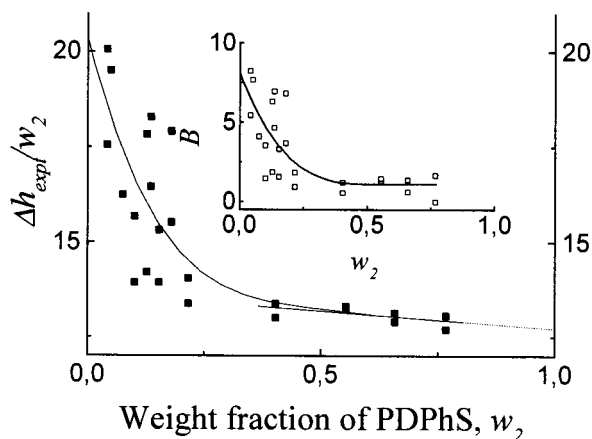


Figure 9. Plots of specific heat of gel melting and gelation h_{exptl}/w_2 , in J g^{-1} , (■) and parameter B , in J cm^{-3} , (□) vs volume fraction of PDPhS in gels (see eqs 6 and 7). Solids curves are calculated using two fitted polynomials: $h_{\text{exptl}}/w_2 = 20.3278 - 47385\phi_2 + 123.23531\phi_2^2 - 145.60494\phi_2^3 - 63.91048\phi_2^4$ and $B = 8.1057 - 41.56018\phi_2 + 86.15139\phi_2^2 - 70.21741\phi_2^3 + 16.17997\phi_2^4$. Dashed line is $h_{\text{exptl}}/w_2 = 13.586 - 0.876\phi_2$.

crystal–mesophase transition $\Delta H_{\text{c-m}}$ and the difference between the enthalpies of the mesophase and the melt at T_{m}° . The latter contribution may be regarded as the apparent heat of isotropization $\Delta H_{\text{i}}^{\circ}$. It is equal to 15.2 J g^{-1} when taking $\Delta H_{\text{c-m}} = 37.0 \text{ J g}^{-1}$ (see above) or to 12.2 J g^{-1} if the reported^{5b} highest value $\Delta H_{\text{c-m}} = 40.0 \text{ J g}^{-1}$ is used.

The value of B can also be assessed using the presented above data on the heats of gelation and melting of gels (Figure 3). The experimentally measured heat of melting (gelation) for a gel sample, h_{exptl} , is made of two contributions, which can be written as

$$h_{\text{exptl}} = h_{\text{fusion}} + h_{\text{mix}} \quad (4)$$

where h_{fusion} is the heat of fusion of the crystalline phase and h_{mix} is the heat of mixing of the molten polymer with the solvent.

As known, the van Laar heat of mixing can be expressed as a function of solvent (ϕ_1) and polymer (ϕ_2) volume fractions and the energy of interaction between molecules of the solvent and the polymer repeat unit. The latter is equated to B (the square of the differences between their solubility parameters) and

$$h_{\text{mix}} = (v_2 + v_1)B\phi_1\phi_2 \quad (5)$$

where v_1 and v_2 are the volumes of solvent and polymer in the sample. It is easily shown, e.g. ref 31, that for a gel with a polymer weight fraction w_2 and density of the melt ρ_2

$$h_{\text{exptl}}/w_2 = h_{\text{fusion}} + \rho_2^{-1}(1 - \phi_2)B \quad (6)$$

$$B = (h_{\text{exptl}}/w_2 - h_{\text{fusion}})\rho_2(1 - \phi_2)^{-1} \quad (7)$$

The plot of h_{exptl} (heats of melting and gelation)/ w_2 against ϕ_2 is shown in Figure 9. The heat of fusion of the PDPhS phase, which exhibits a certain degree of crystallinity, and B can be evaluated from this plot. Linear extrapolation of the right portion of the curve in Figure 9 to $\phi_2 = 1$ yields the heat of fusion of the undiluted PDPhS phase, equal to 12.7 J g^{-1} . This

quantity combines the heats of the crystal–mesophase transition and the above-mentioned transition mesophase–imaginary isotropic melt.

As the heat of crystal–mesophase transition is practically constant for all the dried gels (see Figure 3), their degree of crystallinity is obviously the same. It equals ~ 0.24 when calculated as the ratio of the extrapolated value of $h_{\text{fusion}} = 12.7 \text{ J g}^{-1}$ to the heat of fusion of the undiluted totally crystalline PDPhS (52.2 J g^{-1}). This value of crystallinity is in accord with that (~ 0.28) determined as the ratio between the presented above heats of the crystal–mesophase transition for the dried gels and for the sample crystallized upon slow cooling from the mesomorphic state (10.3 and 37.0 J g^{-1} , respectively).

The second term on the right-hand side of eq 6 characterizes the heat of mixing of amorphous PDPhS with DPhE, expressed in J g^{-1} . As shown above, the crystalline gels of PDPhS possess the lamellar morphology and amorphous domains seem to be located inside of the crystalline lamellae and thus not to be in a direct contact with DPhE molecules. Such occluded amorphous phase is expected to dissolve simultaneously with dissolving the crystalline part of the lamellae, and consequently, the heat of mixing should be related to the overall polymer fraction in the gel.

The plot of h_{exptl}/w_2 vs ϕ_2 is nonlinear, and therefore, B is concentration-dependent. Using eq 7, we have calculated the value of B over the entire range of ϕ_2 taken tentatively $\rho_2 = 1.06 \text{ g cm}^{-3}$ (the mesophase density at 220°C). The plots of h_{exptl}/w_2 and B vs ϕ_2 can be described rather well by two fitted polynomials (see Figure 9), which at $\phi_2 = 0$ give the values of h_{mix} and B at infinite dilution (7.9 J g^{-1} and 8.33 J cm^{-3}). Such a heat of mixing is commensurate with the heat of fusion of the crystalline phase in the gels (12.7 J g^{-1}). The value of B at infinite dilution practically coincides with that estimated above using eq 3. However, with increasing ϕ_2 B does not remain constant but initially drops sharply and then, at $\phi_2 > 0.4$, is striving to level off at a value of $\sim 1.1 \text{ J cm}^{-3}$. Such a concentration dependence of B may reflect changes in the solution structure, which make eqs 5–7 invalid for calculation of B at higher concentrations. It also implies that eq 3 with the constant B is only a certain approximation, and the calculated value of B is likely an average for the whole concentration range.

Mesophase Isotropization. Dissolution of the crystalline phase of gels with $w_2 > 0.8$ occurs in two steps, i.e., via an intermediate stage of the mesophase existence. Therefore, for constructing a complete phase diagram for the PDPhS–DPhE system it is necessary to analyze the influence of solvent on the mesophase isotropization and to draw the corresponding mesophase isotropization (dissolution) line. Such consideration is also useful for an assessment of the temperature range where isotropization of PDPhS would occur in the absence of thermal degradation. Unfortunately, we could gain only very scarce data on the phase behavior of the PDPhS gels at so high polymer concentrations due to a lot of experimental problems (retarded kinetics of dissolving; very high temperatures of dissolution which are in the vicinity and even above the boiling point of DPhE and, as a result, high DPhE vapor pressures that make impossible reliable DSC measurements; temperature restrictions in observation under a microscope).

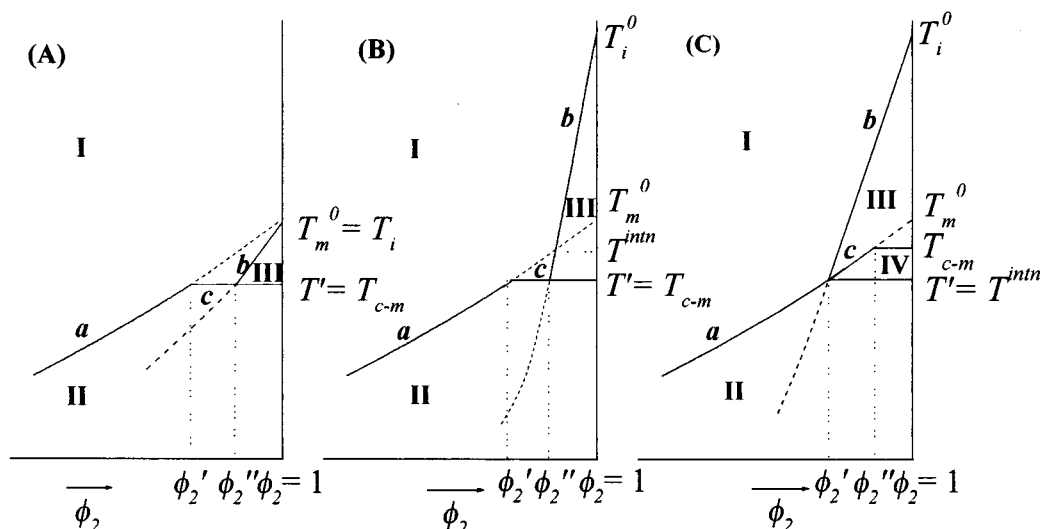


Figure 10. Schematic representation of phase diagrams with interference between crystal melting curve (liquidus line) and mesophase–isotropic solution boundary curve (mesophase dissolution line) for the binary system polymer–solvent, in which the pure polymer undergoes a thermotropic transition crystal–mesophase at temperature T_{c-m} : (A) for flexible-chain polymer with a real isotropization temperature T_i^0 , coinciding with the equilibrium virtual melting point of the crystalline phase T_m^0 to which liquidus line a is extrapolated; (B) and (C) for polymers forming anisotropic melt (mesophase) due to steric interactions of rigid/semirigid chains when temperature of intersection, T^{intn} , of liquidus (a) and mesophase dissolution (b) lines is higher and lower than T_{c-m} , respectively. In both latter cases $T_i^0 > T_m^0$, and if T_i^0 is very high, it can be not attained experimentally due to thermal degradation of the polymer. See text for more detail.

Well-reproducible temperatures of the full dissolution of PDPhS could be measured only up to a polymer weight fraction of 0.85. In the first DSC heating run of the virgin gel with $w_2 = 0.85$ an endotherm was observed in the vicinity of 230 °C. The observation under polarizing microscope showed that in this temperature region crystalline spherulites disappeared completely, but the system remained biphasic; i.e., along with formation of an isotropic solution a birefringent phase (mesophase) persisted (see Figure 7b). Upon further heating the mesophase progressively disappeared in the temperature range of 290–310 °C, and the system became homogeneous. Upon subsequent cooling from 340 °C the formation of the mesophase was observed starting with about 260 °C. This process was followed by crystallization, which manifested itself as a jumpwise increase in birefringence and the appearance of growing spherulites. We have definitely established that the transition from the one-stage to two-stage conversion of the gels into isotropic solutions always occurred in the vicinity of $w_2 = 0.8$. Consequently, we have tentatively taken the point on the crystal melting line corresponding to $w_2 = 0.8$ ($T_m = 233$ °C) as one belonging also to the mesophase isotropization line, i.e., as the point of intersection of these phase boundary curves.

Obviously, the data on the phase behavior for such a narrow range of w_2 as 0.8–0.85 are insufficient for constructing the genuine phase boundary curve dividing the regions of isotropic solutions and mesophase existence. Nevertheless, these data can be useful for a better understanding of the origin of the mesophase in PDPhS. In this connection let us consider qualitatively some types of phase diagram expected for the crystalline polymer–solvent system in which the polymer undergoes a transition crystal I–partially disordered crystal II (in particular, thermotropic mesophase).

The conversion of a 3D crystal, formed by flexible macromolecules, into a thermotropic mesophase (e.g.,

columnar mesophase regarded as 2D crystal) and the existence of the latter in a certain temperature range, before it eventually transforms into isotropic melt, can origin from stepwise releasing with temperature discrete intra- and intermolecular interactions which occur in the 3D crystal and persist in part in the mesophase. For semirigid macromolecules (with a sufficiently high axial ratio of the Kuhn segment) steric factors and the anisotropy of intermolecular interactions can underlie formation of an anisotropic melt (thermotropic mesophase) after melting the antecedent crystalline phase. The generalized phase diagram for the system solvent–crystalline polymer, exhibiting a crystal–mesophase transition, is in principle a result of interference of phase transitions of three types, i.e., solution–crystal, solution–mesophase, and mesophase–crystal transformation.

The different origin of thermotropic mesophases should obviously be reflected in the form of the phase diagram. Figure 10 shows schematically three phase diagrams patterns, which may be proposed for the two marginal types of thermotropic mesophase indicated above. Differences between them can apparently serve as a basis for discrimination between driving forces for the mesophase formation.

If the crystal–mesophase transition in a undiluted crystalline flexible polymer is caused by the disruption of one part of the interactions, existing in the 3D crystal, with the retention of the others in the mesophase and if, at dissolving the 3D crystal, isotropic solutions form in the entire concentration range, one can expect for such a polymer–solvent system phase diagram A shown in Figure 10. In this case the equilibrium virtual melting temperature T_m^0 of the 3D crystal, found by extrapolation of the crystal melting (liquidus) line a to the polymer concentration $\phi_2 = 1$ (the dashed portion of curve a calculated, for instance, using the Flory equation), should conceptually coincide with the isotropization temperature T_i^0 of the pure polymer. Depression

of T_i° in the presence of solvent is expressed in this diagram by the mesophase isotropization (dissolution) line b (its dashed section relates to T_i , which would be observed in the case of suppression of crystallization). In region I and II isotropic solutions and the crystalline phase exist, respectively. At a volume polymer fraction ϕ_2' , the dissolution temperature of the crystalline phase T reaches the temperature of the crystal–mesophase transition T_{c-m} , and further, at $\phi_2 > \phi_2'$, dissolution of the crystalline phase follows its preceding transformation into the mesophase. In the region of polymer concentration from ϕ_2' to ϕ_2'' the dissolution temperature of the mesophase is less than T_{c-m} , and therefore, the observed dissolution temperature of the crystals should remain unchanged and equal to T_{c-m} (horizontal section c of the liquidus line). At the polymer content above ϕ_2'' the isotropization (dissolution) temperature becomes higher than T_{c-m} (curve b), and in region III the mesophase and isotropic solutions coexist.

On dissolving a crystalline phase formed by sufficiently rigid macromolecules, the thermodynamic conditions can arise at a certain concentration of the macromolecules in the solution when an anisotropic polymer phase separates out. (The chain stiffness and polymer–solvent interaction determine this critical concentration.³²) Therefore, the phase diagram for such a binary system should consist of two intersecting phases boundary curves: a liquidus line in the region of low concentrations, and, at higher concentrations, a curve enclosing the region where isotropic solutions and anisotropic ones (pure polymer mesophase as an extreme) coexist.³³

Generally, T_i of the thermotropic mesophase (anisotropic melt) formed by semirigid macromolecules is determined by intermolecular interactions and the axial ratio of the Kuhn segment (steric interactions). According to theory, the nematic order in the athermal melt of macromolecules should occur at the axial ratio of the Kuhn segment equal to ~ 7 .^{34,35} Isotropization of such a mesophase may be expected only if with increasing temperature the axial ratio becomes less than the indicated above value. This can in turn result from increasing flexibility of the macromolecules due to developing intramolecular mobility (decreasing the Kuhn segment) or/and from an increase in their apparent diameter owing to thermal expansion of the melt. The isotropization temperature T_i° of any thermotropic mesophase, formed by rigid or semirigid macromolecules, should be higher than the virtual melting point T_m° of the antecedent crystalline phase (evaluated by extrapolation of the liquidus line on the phase diagram to the polymer concentration $\phi_2 = 1$) as the latter parameter relates to the virtual transition of macromolecules from the crystalline into disordered state but not into an orientationally ordered melt.

In Figure 10 two schematic phase diagrams B and C are presented for the cases when (i) the temperature of the crystal–mesophase transition T_{c-m} is lower than the temperature T^{intn} of an imaginary intersection of liquidus (a) and mesophase dissolution (b) line; (ii) T_{c-m} is above the real T^{intn} .

In the former case the combined phase boundary curve, above which isotropic solutions exist (region I), consists of three sections. These are portion a (liquidus line), which delineates the melting temperatures of the crystalline phase in the presence of solvent; portion b characterizing the temperatures of complete dissolution

of the mesophase (i.e., depression of T_i in the presence of solvent); and horizontal section c extended from ϕ_2' to ϕ_2'' . Within the last section, which is similar to the section c in Figure 10A, the crystalline phase dissolves immediately after conversion into the mesophase at the constant temperature $T = T_{c-m}$. In the phase diagram region II is related to the crystalline phase. In region III isotropic solution and the anisotropic phase (pure mesophase in the given case) coexist.

In the phase diagram C the region of isotropic solutions is bounded by the left portion of liquidus line a and curve b , indicating the depression of T_i in the presence of solvent. These curves intersect at the point corresponding to the temperature T and the polymer volume fraction ϕ_2' above which the complete dissolution of the crystalline polymer proceeds via the intermediate stage of existence of the anisotropic melt. A peculiar feature of this phase diagram is that in subregion IV, which is a part of region II, can coexist three phases, viz. the crystalline phase, isotropic solution, and anisotropic melt. In region III isotropic solutions and the anisotropic melt coexist. Within the range of polymer concentrations from ϕ_2' to ϕ_2'' the temperature, at which the crystalline phase disappears, is elevating along curve c , and above ϕ_2'' it becomes constant and equal to T_{c-m} .

In the PDPhS/DPhE system studied the temperature of complete dissolution of the mesophase even at the polymer concentration $w_2 = 0.85$ ($\phi_2 = 0.825$) is already markedly higher than the extrapolated equilibrium virtual melting point of the antecedent crystalline phase (~ 300 °C against $T_m^\circ = 280$ °C). Hence, the phase diagram of this binary system presented in Figure 2 does not match that shown in Figure 10A. The temperature of intersection of the crystal melting and mesophase isotropization line (233 °C) is lower than T_{c-m} of the dried annealed gels. Thus, the phase diagram of the PDPhS–DPhE system should seemingly be related to that shown in Figure 10C. This fact means that a considerable contribution into the mesophase behavior of PDPhS is apparently originated from a relatively high stiffness of its macromolecules. In principle, this inference is in accord with the above-mentioned results of simulations on PDPhS macromolecules according to which their “characteristic ratio” C equals ~ 65 at room temperature and ~ 30 above 200 °C.²⁴

The observed sharp growth of the temperature of complete dissolution of PDPhS-A from 233 to 300 °C, as its weight fraction in the gels increases from 0.8 only to 0.85, suggests a very high isotropization temperature T_i° of undiluted high molecular weight PDPhS. At the present time there exists no proper theory that describes quantitatively in the explicit form depression of the isotropization temperature in the presence of solvent for mesophases formed by rigid macromolecules. We attempted to assess the equilibrium thermodynamic parameters of isotropization for PDPhS through use of eq 3 although a solid physical basis for its application in this case is absent. The Flory equation is valid for crystalline flexible polymers that produce isotropic melts. Using this equation for description of the concentration dependence of T_i for thermotropic mesophases, which originate from steric interactions of rigid and semirigid chains, means, in essence, that (i) isotropization of the anisotropic melt in the absence of solvent is formally treated as the conventional melting of a flexible-chain polymer crystal and (ii) the enthalpy and

entropy of fusion of such a crystal are equated to the differences between the enthalpies and entropies of the isotropic and anisotropic melt at T_i° .

In the context of our consideration it is necessary to underline the following key difference between the isotropization of mesophases formed by flexible and rigid macromolecules. The high-temperature crystalline modification (mesophase) of flexible polymer would melt theoretically strictly at a single melting point with jumpwise changes of its enthalpy and entropy. In contrast, the transition of the anisotropic melt of a rigid-chain polymer into the isotropic phase should proceed as gradual changes in the orientational parameter characterizing deviations from the parallel arrangement of macromolecules (due to increasing free volume and chain flexibility with temperature). Consequently, the anisotropic melt–isotropic melt transition is anticipated to be accompanied by gradual changes in the enthalpy and entropy of the anisotropic melt within a rather wide temperature interval, and these changes should manifest themselves as an increase in heat capacity. In principle, at the final temperature of the anisotropic melt existence (isotropization temperature), one can also expect a small jump in the enthalpy, which will be determined by the energy of orientation-dependent interactions retained to this temperature.

Therefore, formal application of eq 3 for estimating the thermodynamic characteristics of isotropization of anisotropic melts (mesophases) of semirigid or rigid-chain polymers may yield an apparent heat of isotropization although this transition is in reality not accompanied by any well-defined thermal effect. Note in this connection that the T_i reported for PDPhS oligomers were determined by means of birefringence measurements and could not be monitored in DSC runs.⁹

We have estimated the heat and temperature of the virtual isotropization of the undiluted PDPhS using the following values of T_i for two gel compositions: 300 °C for $w_2 = 0.85$ ($\phi_1 = 0.175$) and 233 °C for $w_2 = 0.8$ ($\phi_1 = 0.231$) (the proposed point of intersection). The estimated values of ΔH_i° and T_i° are 1.72 kJ mol⁻¹ (8.6 J g⁻¹) and 757 °C. We also analyzed how the tentatively chosen position of intersection point can affect the values of the above parameters. For this purpose, ΔH_i° and T_i° were computed varying w_2 of intersection in an experimentally reasonable range from 0.81 to 0.77 and T_i^{intn} from 235 to 228 °C, respectively. ΔH_i° was found to change from 1.41 kJ mol⁻¹ (7.1 J g⁻¹) to 2.39 kJ mol⁻¹ (12.1 J g⁻¹) and T_i from 962 to 565 °C. All the estimated values of ΔH_i° , especially the last one, are in good agreement with 12.2 J g⁻¹ calculated above as the difference between ΔH_m° and ΔH_{c-m}° , taking into account the discussed experimental difficulties in monitoring the dissolution of the crystalline phase and mesophase. Thus, one may suggest that a value of $\Delta H_i^\circ = 12$ J g⁻¹ is close to the real difference between the enthalpies of the mesophase and isotropic melt of PDPhS although the applicability of eq 3 remains open for discussion.

The evaluated values of T_i° turned out to be more sensitive to the chosen location of the intersection point. We compared these values with those obtained by extrapolation of the reported T_i for PDPhS oligomers⁹ to infinite molecular weight (see Figure 11). T_i° was found to be equal to 480 °C (when using all the presented experimental points) or to 550 °C (when

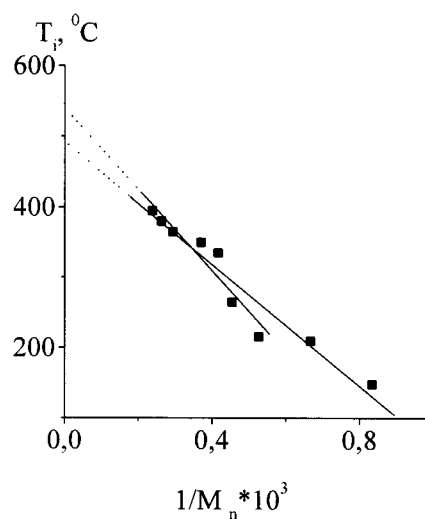


Figure 11. Plots of T_i of PDPhS oligomers (taken from ref 9b) vs the reciprocal of their molecular weight (see text).

excluding the data for the two lowest molecular weight oligomers). Such extrapolation is based on the well-known Thomson–Gibbs equation, which relates the melting point of crystalline lamellae to the reciprocal of their thickness. It was successfully used for estimating the equilibrium melting points of some crystalline polymers (see ref 36 and references therein) and the equilibrium isotropization temperatures of the lamellar mesophases of several flexible polysiloxanes as well.^{37,38}

The validity of this approach to determining T_i° of mesophases formed by semirigid macromolecules is also problematic due to a large input of steric interactions into the free energy of formation of the mesomorphic lamellae. Nevertheless, the value of $T_i = 550$ °C is quite close to 565 °C estimated using eq 3. Therefore, one may assume that in the absence of thermal degradation the isotropization of high molecular weight PDPhS would occur, if at all, in the vicinity of 560 °C or at even higher temperatures.

Concluding Remarks

Thermally reversible crystalline gels of PDPhS formed upon cooling its solutions in DPhE are a prominent example of the peculiar lamellar gel morphology resulting from the specific growth of spherulite-like superstructures whose overlapping yields a three-dimensional skeleton filled with solvent. Although the formation of gels with a similar morphology was already observed earlier for some flexible polymers and according to ref 21, such a morphology is an inherent feature of crystallization of polymers from homogeneous solution without preceding liquid–liquid demixing, this interesting phenomenon has not been adequately investigated. In this paper we presented data that depict the morphological changes to occur in such gels of PDPhS with increasing polymer content and temperature of the gel formation. We also discussed the inner organization of growing crystalline lamellae and the reason for the considerable decrease of their melting point in the gels with low polymer content in terms of temperature and concentration dependence of the critical dimensions of secondary crystalline nuclei.

The binary system PDPhS–DPhE exhibits the complicated phase behavior resulting from the occurrence of the crystal–mesophase transition in pure PDPhS. The phase diagram of this system is an example of as

yet poorly studied interference of two types of phase equilibrium, i.e., crystal–isotropic solution and mesophase–isotropic solution. Besides the experimental difficulties, which we encountered when studied the latter, there exists also a problem of its thermodynamic treatment. We attempted to use the Flory equation for describing depression of the isotropization temperature of the mesophase in the presence of DPhE. However, such an approach is not sufficiently justified, and this problem requires a more detailed consideration.

We have also shown that the melting temperatures of the annealed wet gels of PDPHS can be satisfactorily described by the Flory equation. With the assumption that these temperatures are the equilibrium melting temperatures of the PDPHS crystalline phase in the presence of DPhE, the equilibrium melting point T_m° and apparent heat ΔH_m° of a virtual crystal–isotropic melt transition in the absence of solvent were estimated. However, such a treatment has two shortcomings. First, the values of these parameters were calculated under assumption of the constancy of the parameter B in the Flory equation over the whole concentration range. Second, it would be physically more reasonable (but experimentally very difficult) to use, as the equilibrium melting points of PDPHS in the presence of solvent, the dissolution temperatures of a more perfect crystalline phase which is formed on cooling the annealed mesophase. Therefore, the calculated values of the T_i° and ΔH_i° should be regarded as preliminary and requiring further refinement.

Having compared the extrapolated values of T_m° with T_i° and analyzed various possible phase diagrams for the system solvent–crystalline polymer, exhibiting a thermotropic crystal–mesophase transition, we have inferred that the mesophase behavior of PDPHS can be linked to an extent with a relative high stiffness of its macromolecules. We suggest that the analysis of depression of the melting point of crystalline phases and the isotropization temperature of mesophases in the presence of solvent might be a useful tool for a qualitative assessment of the chain rigidity contribution to the thermotropic mesophase behavior of polymers.

Acknowledgment. This research was supported by the Russian Basic Research Fund (Project 98-03-33329).

References and Notes

- (1) Andrianov, K. A. In *Metalloorganic Polymers*; Bradley, D. C., Ed.; John Wiley & Sons Interscience: New York, 1965.
- (2) (a) Tsvankin, D. Ya.; Levin, V. Yu.; Papkov, V. S.; Zhukov, V. P.; Zhdanov, A. A.; Andrianov, K. A. *Polym. Sci. USSR (Engl. Transl.)* **1979**, *21*, 2348. (b) Ibemezi, J.; Gvozdk, N.; Keumin, M.; Lynch, M. J.; Meier, D. J. *Polym. Prepr.* **1985**, *26*, 18. (c) Lee, M. K.; Meier, D. J. *Polymer* **1993**, *34*, 4882. (d) Harkness, B. R.; Tachikawa, M.; Mita, I. *Macromolecules* **1995**, *28*, 1323.
- (3) (a) Mark, J. E.; Chiu, D. S. *Polym. Prepr.* **1977**, *18*, 481. (b) Falender, J. R.; Yen, G. S.; Chiu, D. S.; Mark, J. E. *J. Polym. Sci., Polym. Phys. Ed.* **1980**, *18*, 389.
- (4) Dubchak, I. A.; Babchinitzer, T. M.; Kazaryan, L. G.; Tartakovskaya, L. M.; Vasilenko, N. G.; Zhdanov, A. A.; Korshak, V. V. *Polym. Sci. USSR (Engl. Transl.)* **1989**, *31*, 70.
- (5) (a) Buzin, M. I.; Gerasimov, M. V.; Obolonkova, E. S.; Papkov, V. S. *J. Polym. Sci., Polym. Chem. Ed.* **1997**, *35*, 1973. (b) Buzin, M. I.; Kvachev, Yu. P.; Svistunov, V. S.; Papkov, V. S. *Vysokomol. Soedin.* **1992**, *B31*, 66.
- (6) Papkov, V. S.; Gerasimov, M. V.; Buzin, M. I.; Il'ina, M. N.; Kazaryan, L. G. *Polym. Sci., Ser. A* **1996**, *38*, 1097.
- (7) Papkov, V. S.; Vasil'ev, V. G.; Buzin, M. I.; Dubovik, I. I.; Il'ina, M. N. *Polym. Sci., Ser. A* **2001**, *43*, 200.
- (8) Buzin, M. I.; Vasilenko, N. G.; Tartakovskaya, L. M.; Zhukov, V. P.; Dubovik, I. I.; Tsvankin, D. Ya.; Papkov, V. S. *Polym. Sci. USSR (Engl. Transl.)* **1990**, *32*, 2242.
- (9) (a) Harkness, B. R.; Tachikawa, M.; Mita, I. *Macromolecules* **1995**, *28*, 8136. (b) Li, L.-J.; Yang, M.-H. *Polymer* **1998**, *39*, 689.
- (10) Flory, P. J. *Principles of Polymer Chemistry*; Cornell University Press: Ithaca, NY, 1953; p 563.
- (11) Guenet, J. *Thermoreversible Gelation of Polymers and Biopolymers*; Academic: London, 1992.
- (12) Te Nijenhuis, K. *Adv. Polym. Sci.* **1997**, *130*, 1.
- (13) Yang, Y. C.; Geil, P. H. *J. Macromol. Sci., Phys.* **1983**, *B22*, 463.
- (14) (a) Shibatani, K. *Polym. J.* **1970**, *1*, 348. (b) Ajasawara, K.; Nakajima, T.; Yamaura, K.; Matsuzawa, S. *Prog. Colloid Polym. Sci.* **1975**, *58*, 145.
- (15) Matsuda, H.; Imaizumi, M.; Fujimatsu, H.; Kuroiwa, S.; Okabe, M. *Polym. J.* **1984**, *16*, 151.
- (16) Tan, H. M.; Chang, B. H.; Baer, E.; Hiltner, A. *Eur. Polym. J.* **1983**, *19*, 1021.
- (17) Takahashi, A. *Polym. J.* **1973**, *4*, 379.
- (18) Aerts, L.; Kunz, M.; Berghmans, H.; Koningsveld, R. *Macromol. Chem.* **1993**, *194*, 2697.
- (19) (a) Giloramo, M.; Keller, A.; Miyasaka, K.; Overbergh, N. *J. Polym. Sci., Polym. Phys. Ed.* **1976**, *14*, 39. (b) Atkins, E. D. T.; Hill, M. J.; Jarvis, D. A.; Keller, A.; Sarhene, E.; Shapiro, J. S. *Colloid Polym. Sci.* **1984**, *262*, 22.
- (20) Lemstra, P. J.; Smith, P. *Br. Polym. J.* **1980**, *12*, 212.
- (21) Mandelkern, L.; Edwards, C. O.; Domszy, R. C.; Davidson, M. W. In *Macromolecules in Polymer Solutions*; Dubin, P., Ed.; Plenum Press: New York, 1985; pp 121–133.
- (22) (a) Tanigami, T.; Suzuki, H.; Yamaura, K.; Matsuzawa, S. *Macromolecules* **1985**, *18*, 2595. (b) Tanigami, T.; En, T.; Yamaura, K.; Matsuzawa, S. *Polym. J.* **1986**, *18*, 31.
- (23) Luman-Heidel, H. *Chem. Met. Eng.* **1934**, *41* (6).
- (24) Patil, R. D.; Mark, J. E. *Comput. Polym. Sci.* **2000**, *10*, 189.
- (25) Jackson, J. B.; Flory, P. J.; Chainy, R. *Trans. Faraday Soc.* **1963**, *59*, 1906.
- (26) Wunderlich, B. *Macromolecular Physics*; Academic Press: New York, 1980; Vol. 3, Chapter 9.
- (27) Hosemann, R. *J. Appl. Phys.* **1963**, *34*, 25.
- (28) Hoffman, J. D.; Davis, G. T.; Lauritzen, J. I., Jr. In *Treatise on Solid State Chemistry*; Hanmay, N. B., Ed.; Plenum Press: New York, 1976; Vol. 3, Chapter 7.
- (29) Hoffman, J. D.; Weeks, J. J. *J. Res. Natl. Bur. Stand.* **1962**, *A66*, 3.
- (30) (a) Takahashi, A.; Nakamura, T.; Kagawa, I. *Polym. J.* **1972**, *3*, 207. (b) Takahashi, A.; Sakai, M.; Kato, T. *J. Polym. J.* **1980**, *12*, 335.
- (31) Phuong-Nguen, H.; Delmas, G. *Macromolecules* **1985**, *18*, 1235.
- (32) Flory, P. J. *Adv. Polym. Sci.* **1984**, *59*, 1.
- (33) Papkov, V. S. *Adv. Polym. Sci.* **1984**, *59*, 25.
- (34) Flory, P. J.; Ronca, G. *Mol. Cryst. Liq. Cryst.* **1979**, *54*, 289, 311.
- (35) Khokhlov, A. R.; Semenov, A. N. *Macromolecules* **1986**, *19*, 373.
- (36) Wunderlich, B. *Macromolecular Physics*; Academic Press: New York, 1980; Vol. 3, Chapter 8.
- (37) Godovsky, Yu. K.; Papkov, V. S. *Adv. Polym. Sci.* **1989**, *88*, 129.
- (38) Molenberg, A.; Moeller, M. *Macromolecules* **1997**, *30*, 8332.

MA0109673